Impact of Channel Non-Reciprocity in Cell-Free Massive MIMO

Jorge Morte Palacios, Orod Raeesi, Ahmet Gokceoglu, and Mikko Valkama, *Senior Member, IEEE*

***Abstract*—In cell-free (CF) massive MIMO, a large number of access points (APs) distributed over the coverage area jointly serve a set of users over the same time/frequency resources. In this paper, we study the impact of channel non-reciprocity (NRC) and imperfect channel state information in CF massive MIMO systems. We derive analytical expressions of capacity lower bounds, including a physically inspired non-reciprocal channel model where the NRC variables vary slowly in time. The conclusion is that under conjugate beamforming, the achievable downlink rate is only sensitive to AP side phase non-reciprocity, hence the calibration requirements can be less restrictive since only the phase reciprocity errors have to be corrected. These findings are new compared to the existing literature where the NRC variables are commonly assumed to be of fast-fading nature.**

***Index Terms*—Cell-free massive MIMO, channel reciprocity, conjugate beamforming, frequency response mismatch, maximum-ratio processing, channel hardening.**

I. Introduction

THIS letter considers a cell-free (CF) massive MIMO system where a large number of randomly distributed access points (APs) are jointly serving a smaller number of spatially multiplexed users [1], through distributed beamforming. The CF notion implies that the network side antennas are spatially dispersed over different APs, instead of being collocated in a single base-station at the centre of the cell or coverage area. The main advantage of the CF massive MIMO concept is the spatial diversity, i.e., the distance between a user and the nearest AP is generally reduced [2]. Such CF massive MIMO deployment has been shown to, e.g., provide more uniform coverage to users at random locations than the corresponding cell-based massive MIMO systems [3].

A time-division duplexing (TDD) network is considered, where uplink pilots or training signals are used for UE-AP channel estimation [3], [4]. Then, building on the channel reciprocity assumption, the APs calculate the downlink precoding or beamforming weights for the actual downlink data transmission [4]. However, although the physical propagation channels were purely reciprocal, the inherent frequency response mismatches of the involved transmitters and receivers and hence the effective UL and DL channels are known to be non-reciprocal [5]. Such TDD-MIMO non-reciprocity (NRC) problem has been considered in the existing literature, in more ordinary centralized MIMO context in [5]–[8], while the distributed case was addressed to a certain extent in [9], [10]. For generality, it is also noted that massive MIMO systems are subject to other challenges, such as pilot contamination [3], [11], however, in this letter we focus on NRC.

J. Morte Palacios and M. Valkama are with Tampere University, Finland.
O. Raeesi is with Nokia Mobile Networks, Finland.
A. Gokceoglu is with Huawei Technologies, Sweden.

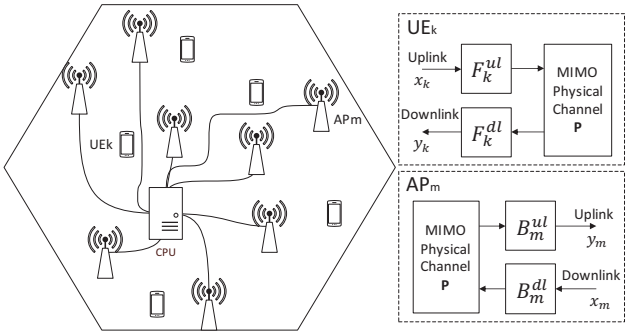

Fig. 1: Illustration of the considered cell-free massive MIMO system with channel non-reciprocity stemming from the frequency response mismatches.

In general, the transceiver frequency response characteristics depend on the hardware implementation and the operating conditions, e.g., temperature drift. Thus, the NRC characteristics vary slowly in time compared with the changes in the physical propagation channel. Therefore, the NRC variables can be assumed to be constant over many propagation channel coherence intervals [10], [12]–[14], and thus the NRC estimation and calibration is commonly executed fairly infrequently, e.g., once in an hour [10], [12], [13]. However, the majority of the performance analysis studies related to NRC analytically model the calibration errors as fast-varying random variables, primarily for analytical tractability [6]–[9]. To address this inconsistency and to provide analysis results with physical basis and practical impact, we consider a more physically-inspired and measurement-based NRC modeling in our analytical derivations, where the NRC values change substantially slower in time. Under such assumption, and considering the implementation-feasible conjugate beamforming processing at the APs together with statistical beamformed channel based detection at UEs, we derive an analytical lower bound for the achievable downlink rate. Different to the previous works [6], [9], [12], the obtained results show that under the above assumptions, the UE side NRC does not affect the CF massive MIMO system performance in any way. Additionally, the results show that system performance is sensitive to AP side phase NRC while amplitude mismatches at AP do not have any essential impact. These findings are clearly new and different from [6]–[9], stemming from the more physically-inspired NRC modeling, and thus provide new information and understanding, e.g., for reciprocity calibration in massive MIMO systems.

II. System Model

A. Basic Assumptions

The basic considered system scenario is shown in Fig. 1. A central processing unit (CPU) controls all the APs, providing

the data payload and signaling needed for synchronized downlink transmission. All the protocols between APs and CPU are excluded from this work, considering a perfect and error-free backhaul with unlimited capacity. We denote the number of APs by M, and the number of users served at the same time-frequency resource by K, while each AP and UE is assumed to be equipped with a single antenna for simplicity.

Building on the TDD principle and channel reciprocity assumption, the APs receive uplink training or pilot sequences from the users to estimate UE-AP channels, and then precode the downlink payload based on the estimates. For simplicity, we assume that there is no pilot contamination which means that users transmit pairwise orthogonal pilot signals, and the uplink training time in symbols, denoted by τ_p, is equal to K. Similar assumptions are made, e.g., in classical works [4], [6], [9]. We do not consider pilot contamination [3], [11] because this work specifically focuses on the impact of channel non-reciprocity. Finally, an OFDM based system is considered, and thus all the upcoming effective channel models are interpreted at an arbitrary passband subcarrier of the system.

B. Non-Reciprocal Channel Modelling

The *effective channels* in downlink and uplink, comprising the effects of both the physical propagation as well as the involved transmitter and receiver hardware, are mutually different since the analog circuitries in the TX/RX paths are formed by different non-ideal components. We model the differences between the effective channels in uplink and downlink, similar to [6], [7], [12], as $\mathbf{G}^{\mathrm{ul}} = \mathbf{B}^{\mathrm{ul}}\mathbf{P}\mathbf{F}^{\mathrm{ul}}$ and $\mathbf{G}^{\mathrm{dl}} = \mathbf{F}^{\mathrm{dl}}\mathbf{P}^{\mathrm{T}}\mathbf{B}^{\mathrm{dl}}$, where $\mathbf{G}^{\mathrm{ul}} \in \mathbb{C}^{M\times K}$ and $\mathbf{G}^{\mathrm{dl}} \in \mathbb{C}^{K\times M}$ are the effective uplink and downlink channel matrices, respectively, $\mathbf{F} = \mathrm{diag}(F_1, ..., F_K)$ and $\mathbf{B} = \mathrm{diag}(B_1, ..., B_M)$ are the diagonal frequency response matrices at the UE and AP sides, respectively, and $\mathbf{P} \in \mathbb{C}^{M\times K}$ is the reciprocal physical MIMO channel matrix. Based on this, we can thus obtain a direct relation between the effective uplink and downlink channels as $g^{\mathrm{dl}}_{mk} = \frac{F^{\mathrm{dl}}_k B^{\mathrm{dl}}_m}{F^{\mathrm{ul}}_k B^{\mathrm{ul}}_m} g^{\mathrm{ul}}_{mk}$.

The physical propagation channels are modeled, similar to [1]–[3], as $p_{mk} = \sqrt{\beta_{mk}} h_{mk}$ where β_{mk} is the large-scale fading coefficient while h_{mk} denotes the small-scale fading. We assume that h_{mk} are independent and identically distributed (i.i.d) $\mathcal{CN}(0, 1)$ random variables (RVs).

The randomness of the transceiver frequency responses is, in turn, captured by the statistics of $\mathbf{B}$ and $\mathbf{F}$. For modeling purposes, we consider that the passband amplitude and phase responses are independent [8], and hence express B_m as

$$B^{\mathrm{x}}_m = A^{\mathrm{x}}_{B_m} e^{j\theta^{\mathrm{x}}_{B_m}} \tag{1}$$

where $x \in \{\mathrm{dl}, \mathrm{ul}\}$, with A and θ denoting the values of the amplitude response and phase response, respectively. Similarly, the frequency responses at the UEs can be denoted as

$$F^{\mathrm{x}}_k = A^{\mathrm{x}}_{F_k} e^{j\theta^{\mathrm{x}}_{F_k}} \tag{2}$$

Let us then denote with σ^2_A the variance of the amplitude responses and with σ^2_θ the variance of the phase responses. In order to model and quantify the reciprocity level of the transceivers, we next define the covariances between the uplink and downlink amplitude and phase responses as

$$\mathrm{Cov}(A^{\mathrm{dl}}_{F_k}, A^{\mathrm{ul}}_{F_k}) = \nu_{A_{\mathrm{UE}}}\sigma^2_A \tag{3}$$
$$\mathrm{Cov}(A^{\mathrm{dl}}_{B_m}, A^{\mathrm{ul}}_{B_m}) = \nu_{A_{\mathrm{AP}}}\sigma^2_A \tag{4}$$
$$\mathrm{Cov}(\theta^{\mathrm{dl}}_{F_k}, \theta^{\mathrm{ul}}_{F_k}) = \nu_{\theta_{\mathrm{UE}}}\sigma^2_\theta \tag{5}$$
$$\mathrm{Cov}(\theta^{\mathrm{dl}}_{B_m}, \theta^{\mathrm{ul}}_{B_m}) = \nu_{\theta_{\mathrm{AP}}}\sigma^2_\theta \tag{6}$$

where ν denotes the relative reciprocity level. Specifically, when $\nu = 1$, the corresponding responses in the uplink and downlink are the same, i.e., the channel is purely reciprocal. Then, the mean squared error (MSE) quantifying the level of non-reciprocity can be expressed as

$$\varepsilon^2_{A_{\mathrm{UE}}} = \mathrm{E}\{|A^{\mathrm{dl}}_{F_k} - A^{\mathrm{ul}}_{F_k}|^2\} = (1 - \nu_{A_{\mathrm{UE}}})\sigma^2_A \tag{7}$$
$$\varepsilon^2_{A_{\mathrm{AP}}} = \mathrm{E}\{|A^{\mathrm{dl}}_{B_m} - A^{\mathrm{ul}}_{B_m}|^2\} = (1 - \nu_{A_{\mathrm{AP}}})\sigma^2_A \tag{8}$$
$$\varepsilon^2_{\theta_{\mathrm{UE}}} = \mathrm{E}\{|\theta^{\mathrm{dl}}_{F_k} - \theta^{\mathrm{ul}}_{F_k}|^2\} = (1 - \nu_{\theta_{\mathrm{UE}}})\sigma^2_\theta \tag{9}$$
$$\varepsilon^2_{\theta_{\mathrm{AP}}} = \mathrm{E}\{|\theta^{\mathrm{dl}}_{B_m} - \theta^{\mathrm{ul}}_{B_m}|^2\} = (1 - \nu_{\theta_{\mathrm{AP}}})\sigma^2_\theta \tag{10}$$

III. Performance Analysis

A. Uplink Channel Estimation

Transceiver frequency responses vary, in general, very slowly in time compared to the corresponding variations in the propagation channel [13], [15]. Thus, we can assume that $\mathbf{B}$ and $\mathbf{F}$ remain constant over many channel coherence intervals. Hence, we define the DL and UL long-term channel power gains as

$$\begin{aligned}\Delta^{\mathrm{dl}}_{mk} &\triangleq \mathrm{E}\{|g^{\mathrm{dl}}_{mk}|^2\} = |F^{\mathrm{dl}}_k|^2\,|B^{\mathrm{dl}}_m|^2 \cdot \beta_{mk}\\ \Delta^{\mathrm{ul}}_{mk} &\triangleq \mathrm{E}\{|g^{\mathrm{ul}}_{mk}|^2\} = |F^{\mathrm{ul}}_k|^2\,|B^{\mathrm{ul}}_m|^2 \cdot \beta_{mk}\end{aligned} \tag{11}$$

and assume that $\Delta^{\mathrm{ul}}_{mk}$ is known when computing below the UL MMSE channel estimate.

To perform the channel estimation, all the UEs simultaneously transmit pairwise orthogonal UL pilot sequences, similar to classical works [3], [4]. We denote the pilot sequence length in samples by τ_p, and let ρ_u denote the uplink normalized signal-to-noise ratio (SNR). The received pilot signal samples in the m-th AP, expressed as a $\tau_p \times 1$ vector, thus read [3]

$$\mathbf{y}_{p,m} = \sqrt{\tau_p \rho_u} \sum_{k=1}^{K} g^{\mathrm{ul}}_{mk} \boldsymbol{\varphi}_k + \mathbf{w}_{p,m} \tag{12}$$

where $\sqrt{\tau_p}\boldsymbol{\varphi}_k \in \mathbb{C}^{\tau_p \times 1}$ is the pilot sequence used by the k-th UE, and $\mathbf{w}_{p,m}$ are i.i.d $\mathcal{CN}(0, 1)$ RVs representing thermal noise. Each AP correlates or de-spreads the received signal by projecting over the pilot sequences, obtaining samples proportional to the channel from the AP to the k-th user. The MMSE estimate of g^{ul}_{mk} is then given by [1], [3]

$$\hat{g}^{\mathrm{ul}}_{mk} = \frac{\mathrm{Cov}(g^{\mathrm{ul}}_{mk}, \check{y}_{p,mk})}{\mathrm{Var}(\check{y}_{p,mk})} \check{y}_{p,mk} = \frac{\sqrt{\tau_u \rho_u}\Delta^{\mathrm{ul}}_{mk}}{\tau_u \rho_u \Delta^{\mathrm{ul}}_{mk} + 1} \check{y}_{p,mk} \tag{13}$$

where $\check{y}_{p,mk} = \boldsymbol{\varphi}^H_k \mathbf{y}_{p,m}$. The corresponding uplink channel estimate variance, denoted by γ_{mk}, reads

$$\gamma_{mk} = \mathrm{E}\{|\hat{g}^{\mathrm{ul}}_{mk}|^2\} = \frac{\tau_u \rho_u (\Delta^{\mathrm{ul}}_{mk})^2}{\tau_u \rho_u \Delta^{\mathrm{ul}}_{mk} + 1} \tag{14}$$

B. Downlink Data Transmission

The APs are assumed to rely on channel reciprocity and thus use the uplink channel estimates directly as the corresponding downlink channel estimates. The downlink multiuser transmit signal is, in general, given by

$$\mathbf{x} = \mathbf{U}\mathbf{q} \tag{15}$$

where $\mathbf{U} = [\mathbf{u}_1, ..., \mathbf{u}_K]$ is the precoding matrix and $\mathbf{q} \in \mathbb{C}^{K\times 1}$ is the normalized symbol vector with $\mathrm{E}\{\mathbf{q}\mathbf{q}^H\} = \mathbf{I}_K$. The matched filter (MF) or maximum ratio transmission (MRT) precoder is obtained by setting $\mathbf{u}_k = [\eta_{1k}^{1/2}\hat{g}_{1k}^{*\mathrm{ul}}, ..., \eta_{Mk}^{1/2}\hat{g}_{Mk}^{*\mathrm{ul}}]^T$ where η_{mk} is the power control coefficient from the m-th AP to the k-th user. The corresponding received signal at the k-th user can then be expressed as

$$r_k = \mathbf{x}^{\mathrm{T}}\mathbf{g}_k^{\mathrm{dl}} + w_k \tag{16}$$

where $w_k \backsim \mathcal{CN}(0,1)$ denotes receiver thermal noise with variance normalized to one.

For presentation simplicity, no specific power control scheme is considered in this work. All APs are assumed to transmit with the same power, and thus the corresponding normalized downlink transmit SNR reads $\rho_d = \mathrm{E}\{|x_m|^2\}$. Hence, at the m-th AP the power control coefficients for all users are equal, i.e. $\eta_{mk} = \frac{\rho_d}{(\sum_{k'=1}^{K}\gamma_{mk'})}$ [3]. We also note that due to the frequency response variations, the actual power radiated at the m-th AP varies accordingly. We adopt this approach because including the frequency response characteristics in the power constraints is likely to be anyway unfeasible in practical systems.

Based on (16), we next separate the desired signal beamformed to the k-th user and the inter-user interference (IUI), as

$$r_k = \mathbf{u}_k^{\mathrm{T}}\mathbf{g}_k^{\mathrm{dl}} q_k + \sum_{k'\neq k}^{K} \mathbf{u}_{k'}^{\mathrm{T}}\mathbf{g}_k^{\mathrm{dl}} q_{k'} + w_k \tag{17}$$

Classical massive MIMO systems [3], [4] are commonly assumed to rely on channel hardening when detecting the received signal, i.e., users rely on the statistics of the beamformed channel to detect the desired symbol. Based on this and the expression in (17), we thus define the desired signal as

$$\mathrm{DS}_k = \mathrm{E}\{\mathbf{u}_k^{\mathrm{T}}\mathbf{g}_k^{\mathrm{dl}}\} q_k \tag{18}$$

Then, the lack of knowledge of the beamformed instantaneous channel, $\mathbf{u}_k^{\mathrm{T}}\mathbf{g}_k^{\mathrm{dl}}$, is captured by the self-interference given by

$$\mathrm{SI}_k = (\mathbf{u}_k^{\mathrm{T}}\mathbf{g}_k^{\mathrm{dl}} - \mathrm{E}\{\mathbf{u}_k^{\mathrm{T}}\mathbf{g}_k^{\mathrm{dl}}\}) q_k \tag{19}$$

Additionally, based on (17), the inter-user interference reads

$$\mathrm{IUI}_k = \sum_{k'\neq k}^{K} \mathbf{u}_{k'}^{\mathrm{T}}\mathbf{g}_k^{\mathrm{dl}} q_{k'} \tag{20}$$

In general, there are many expressions and bounds to analyze the achievable downlink rate [16]. The so-called Use-and-then-Forget (UatF) [17] is a simple lower bound, which in most centralized Massive MIMO cases is also tight. This bound is computed using the effective SINR as [17]

$$R_k^{\mathrm{UatF}} = \log_2(1 + \mathrm{SINR}_k) \tag{21}$$

where SINR_k, considering the interference terms as uncorrelated effective noise, is defined as follows

$$\mathrm{SINR}_k = \frac{\mathrm{E}\{|\mathrm{DS}_k|^2\}}{\mathrm{E}\{|\mathrm{SI}_k|^2\} + \mathrm{E}\{|\mathrm{IUI}_k|^2\} + 1} \tag{22}$$

We next compute the three terms separately following a similar approach as in [3], which yields

$$\mathrm{E}\{|\mathrm{DS}_k|^2\} = \left| \sum_{m=1}^{M} \eta_{mk}^{1/2}\gamma_{mk} \frac{F_k^{\mathrm{dl}} B_m^{\mathrm{dl}}}{F_k^{\mathrm{ul}} B_m^{\mathrm{ul}}} \right|^2 \tag{23}$$

$$\mathrm{E}\left\{|\mathrm{SI}_k|^2\right\} = \sum_{m=1}^{M} \eta_{mk}\Delta_{mk}^{\mathrm{dl}}\gamma_{mk} \tag{24}$$

$$\mathrm{E}\left\{|\mathrm{IUI}_k|^2\right\} = \sum_{m=1}^{M} \Delta_{mk}^{\mathrm{dl}} \sum_{k'\neq k}^{K} \eta_{mk'}\gamma_{mk'} \tag{25}$$

The final expression of the effective SINR is thus given by

$$\mathrm{SINR}_k = \frac{\left| \sum_{m=1}^{M} \eta_{mk}^{1/2}\gamma_{mk} \frac{F_k^{\mathrm{dl}} B_m^{\mathrm{dl}}}{F_k^{\mathrm{ul}} B_m^{\mathrm{ul}}} \right|^2}{\sum_{m=1}^{M} \Delta_{mk}^{\mathrm{dl}} \sum_{k'=1}^{K} \eta_{mk'}\gamma_{mk'} + 1} \tag{26}$$

We note that these expressions capture both the effects of uplink based channel estimation as well as the non-reciprocity due to transceiver frequency response mismatches.

C. Impact of Non-Reciprocity with Perfect Channel Estimation

Next, we consider the particular case of perfect channel estimation at the AP side, to simplify the general analytical expressions, and to obtain insight on the effects of the NRC alone. The uplink channel estimate power reads now $\gamma_{mk} = \Delta_{mk}^{\mathrm{ul}}$, while the desired signal power or the beamforming gain and the self-interference plus IUI power are given by

$$\mathrm{E}\{|\mathrm{DS}_k|^2\} = |F_k^{\mathrm{ul}}|^2 |F_k^{\mathrm{dl}}|^2 \left| \sum_{m=1}^{M} \eta_{mk}^{1/2} \frac{|B_m^{\mathrm{ul}}|^2}{B_m^{\mathrm{ul}}} \beta_{mk} B_m^{\mathrm{dl}} \right|^2 \tag{27}$$

$$\mathrm{E}\left\{|\mathrm{SI}_k|^2\right\} + \mathrm{E}\left\{|\mathrm{IUI}_k|^2\right\} = \sum_{m=1}^{M} |F_k^{\mathrm{dl}}|^2 |B_m^{\mathrm{dl}}|^2 \beta_{mk} \sum_{k'=1}^{K} \eta_{mk'} |F_{k'}^{\mathrm{ul}}|^2 |B_m^{\mathrm{ul}}|^2 \beta_{mk'} \tag{28}$$

1) Impact of UE side NRC: Based on (27) and (28), we can observe that only the UE side amplitude response appears in the expressions. Hence, the phase non-reciprocity at UEs does not degrade system performance. Specifically, the interference terms in (28) only contain the product of the transceiver frequency responses, thus a non-reciprocal response at UE side does not increase the interference power. Additionally, the amplitude non-reciprocity is not present in (27) either, but the product of both uplink and downlink amplitude responses, implying that a non-reciprocal response does not reduce the beamforming gain. The frequency responses variations can thus be seen as gain errors which do not cause IUI.

2) Impact of AP side NRC: From (27), we observe that the amplitude mismatch at the AP side does not reduce the beamforming gain since the uplink frequency response at the AP, B_m^{ul}, is effectively normalized in amplitude. However, based on (27), the phase reciprocity errors at the AP side will impact

the beamforming direction, i.e., the transmitted signals from each AP to the k-th user do not add up purely coherently anymore, reducing the beamforming gain. Regarding the impact on the inter-user interference in (28), only the product of the transceiver frequency responses is present, hence, a non-reciprocal response does not increase the IUI power.

Based on the analytical results and above discussion, we can thus conclude that

- the UE side phase and amplitude non-reciprocity do not degrade the performance;
- the AP side amplitude non-reciprocity does not degrade the performance;
- the AP side phase non-reciprocity degrades the performance because the simultaneous transmit signals do not anymore add up coherently at the receiver

We note that these conclusions are valid under the assumption of conjugate or MRT beamforming at APs, which is the most common assumption in CF massive MIMO systems [1]–[3]. For generality, it is also noted that a similar conclusion regarding MRT precoder sensitivity to channel amplitude impairments due to pilot contamination is drawn in [11].

D. Channel Hardening and Non-Reciprocal Channels

Previous works show that CF massive MIMO systems may, in general, suffer from lack of channel hardening [18]. In this letter, we assume that UEs only use statistical beamformed channel knowledge when detecting the received signal because it is a feasible and practical approach. In contrast to works assuming a fast-varying NRC model [5]–[8], [12], the analytical results presented in this letter show that the beamforming gain uncertainty does not increase under non-reciprocal channel conditions and MRT precoding. Specifically, the gain uncertainty with a perfect channel estimate is given by

$$\mathrm{Var}(\mathbf{u}_k^{\mathrm{T}}\mathbf{g}_k^{\mathrm{dl}}) = \sum_{m=1}^{M} \eta_{mk} |F_k^{\mathrm{ul}}|^2 |F_k^{\mathrm{dl}}|^2 |B_m^{\mathrm{ul}}|^2 |B_m^{\mathrm{dl}}|^2 \beta_{mk}^2 \qquad (29)$$

which does not depend on the reciprocity error ratio but on the product of the transceiver responses. Thus, since UEs use the expected value of the beamformed channel to detect the data, NRC effects are captured in that statistical moment because NRC values vary slowly compared to variations in the physical channel [13], [15]. Hence, in our system model, since the level of NRC does not increase the beamforming gain uncertainty, it does not obstruct channel hardening. On the contrary, in works assuming fast-varying NRC models [5]–[8], [12], the beamforming gain uncertainty increases because UE NRC values are assumed to be different and random between consecutive coherence intervals, entailing that the beamformed channel does not harden.

IV. Numerical Results and Discussions

In this section, we analyze a system where 100 APs and 20 users are uniformly and independently distributed over the coverage area of 1×1 km^2, operating at 1.9 GHz. The large-scale coefficients β_{mk} are modeled following the 3GPP LOS/NLOS Urban Micro path-loss model [19]. The basic evaluation parameters are summarized in Table I.

TABLE I: Basic evaluation parameters

Parameter	Value
Number of APs, M	100
Number of users, K	20
UL pilot length, τ_p	20
Centre frequency, f_c	1.9 GHz
Bandwidth	20 MHz
Transmit powers, $\bar{\rho}_d$, $\bar{\rho}_u$	100 mW, 100 mW
Antenna heights, AP, UE	10 m, 1.65 m
RX noise figure	9 dB

For evaluation simplicity and to have reproducible results, we model the amplitudes of the frequency responses $\{A_{F_k}^{\mathrm{dl}} A_{F_k}^{\mathrm{ul}} A_{B_m}^{\mathrm{dl}} A_{B_m}^{\mathrm{ul}}\}$ as uniform random variables on the range $[1-\epsilon, 1+\epsilon]$, where ϵ is chosen to set $\sigma_A^2 = 0.01$. Additionally, the phases of the frequency responses $\{\theta_{F_k}^{\mathrm{dl}} \theta_{F_k}^{\mathrm{ul}} \theta_{B_m}^{\mathrm{dl}} \theta_{B_m}^{\mathrm{ul}}\}$ are uniformly distributed on the range $[-\pi, \pi)$, that implies a phase variance of $\sigma_\theta^2 = (2\pi)^2/12$ rad^2, while the actual root mean squared phase error is controlled by $\nu_{\theta_{\mathrm{AP}}}$ and $\nu_{\theta_{\mathrm{UE}}}$.

To assess and compare the system performance under different non-reciprocity levels, we use the CDF of the per-user rate as a metric and specifically the corresponding 5th and 95th percentiles. One thousand random realizations are considered, such that for each realization, we generate a set of UE and APs positions and non-reciprocity realizations, and we apply (26) to compute the effective SINR.

In Fig. 2, we compare the per-user rate CDFs for different non-reciprocity sources, such that other sources are deliberately set to zero. In these evaluations, transceiver frequency responses in uplink and downlink are uncorrelated when non-reciprocity is considered, i.e., $\nu = 0$. As can be observed in Fig. 2(a), the system is only sensitive to phase non-reciprocity at APs, confirming the insight obtained through the analytical results already in Section III. Additionally, we observe that the assumed amount of AP side phase NRC has a significant impact on both the 5th and 95th percentiles.

For comparison, Fig. 2(b) shows also the corresponding rate results under fast-varying NRC assumption used in [5]–[8], [12]. As can be observed, the UE side NRC under the fast-varying model degrades system performance even more than the AP side NRC. Additionally, a given amount of AP side NRC degrades the system performance more under the fast-varying model compared to the slow-varying one. We can thus state that the conclusions obtained through the fast-varying model are largely different compared to the physically-inspired slow-varying NRC model considered in this letter, and that the fast-varying models generally overestimate the NRC impacts, since the drifting in true transceiver hardware is slow.

To further quantify the performance degradation under phase non-reciprocity at APs, Fig. 3 shows the 5th and 95th percentiles of the per-user rate CDF for varying level of the phase non-reciprocity RMSE. We observe that CF massive MIMO systems tolerate AP side phase errors of up to 15° without substantially degrading the performance, however, above that level, the system performance is critically degraded.

V. Conclusion

In this letter, we analyzed the performance of MRT precoding based CF massive MIMO systems under physically-inspired

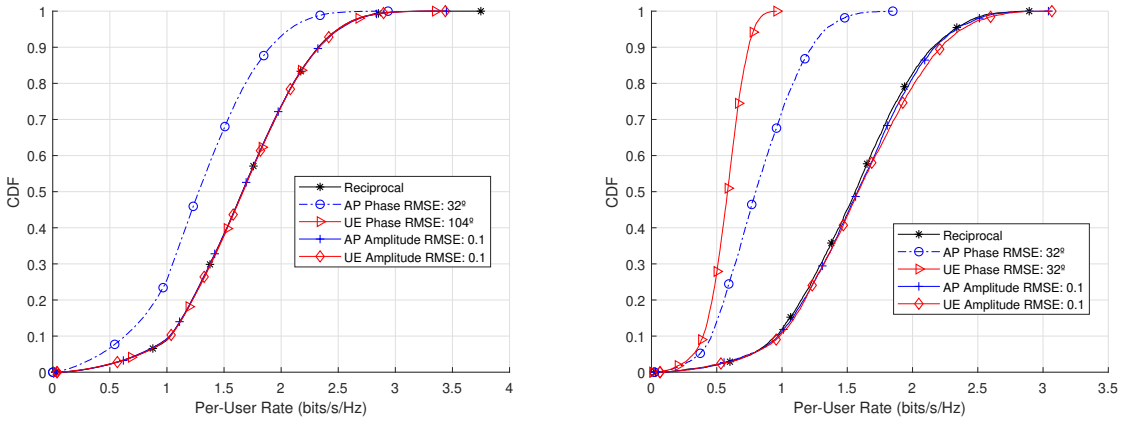

(a) slow-varying model (b) fast-varying model

Fig. 2: CDFs of the per-user rate under different non-reciprocity sources, with (a) slow-varying and (b) fast-varying NRC models. When a certain non-reciprocity source is considered, the others are deliberately set to zero.

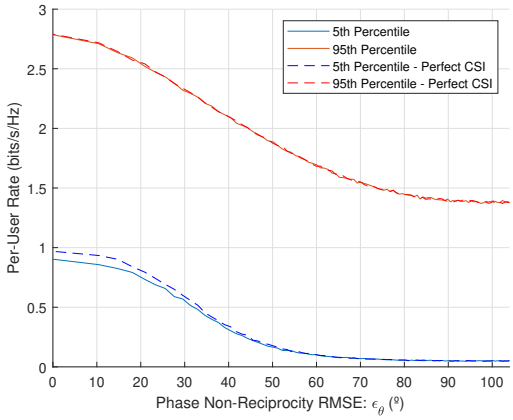

Fig. 3: Per-user rate in the presence of AP side phase NRC, slow-varying NRC model. Other non-reciprocity sources are assumed ideal.

slow-varying channel non-reciprocity, while also considering imperfect channel estimation. When the UEs utilize the statistical beamformed channel knowledge for data decoding, the obtained analytical and numerical results show that only the phase NRC at the AP side degrades the performance, while the UE side NRC does not affect the system performance. These findings are new and different compared to the existing NRC analysis results building on fast-varying NRC models, and indicate that the reciprocity calibration processes can in practice be optimized to focus on estimating and compensating for the phase errors at APs. Extending the analysis to other precoding schemes constitutes an important topic for future work.

REFERENCES

[1] H. Q. Ngo, A. Ashikhmin, H. Yang, E. G. Larsson, and T. L. Marzetta, "Cell-Free Massive MIMO: Uniformly great service for everyone," in *Proc. IEEE SPAWC 2015*, Stockholm, Sweden, Jun. 2015, pp. 201–205.

[2] E. Nayebi, A. Ashikhmin, T. L. Marzetta, and H. Yang, "Cell-Free Massive MIMO systems," in *2015 49th Asilomar Conf. on Signals, Syst. and Comput.* Pacific Grove, CA, USA: IEEE, Nov. 2015, pp. 695–699.

[3] H. Quoc, A. Ashikhmin, H. Yang, and E. G. Larsson, "Cell-Free Massive MIMO Versus Small Cells," *IEEE Trans. Wireless Commun.*, vol. 16, pp. 1834–1850, Mar. 2017.

[4] H. Q. Ngo and E. G. Larsson, "No Downlink Pilots Are Needed in TDD Massive MIMO," *IEEE Trans. Wireless Commun.*, vol. 16, no. 5, pp. 2921–2935, May 2017.

[5] X. Luo, "How Accurate Calibration Is Needed in Massive MIMO?" in *Proc. 2015 IEEE Globecom Workshops*, Dec. 2015, pp. 1–6.

[6] O. Raeesi, A. Gokceoglu, Y. Zou, E. Bjoernson, and M. Valkama, "Performance Analysis of Multi-User Massive MIMO Downlink Under Channel Non-Reciprocity and Imperfect CSI," *IEEE Trans. Commun.*, vol. 66, pp. 2456–2471, Jun. 2018.

[7] Y. Zou, O. Raeesi, R. Wichman, A. Tolli, and M. Valkama, "Analysis of Channel Non-Reciprocity Due to Transceiver and Antenna Coupling Mismatches in TDD Precoded Multi-User MIMO-OFDM Downlink," in *Proc. IEEE VTC 2014*, Vancouver, BC, Canada, Sep. 2014.

[8] D. Mi *et al.*, "Massive MIMO Performance With Imperfect Channel Reciprocity and Channel Estimation Error," *IEEE Trans. Commun.*, vol. 65, no. 9, pp. 3734–3749, Sep. 2017.

[9] A. Minasian, S. Shahbazpanahi, and R. S. Adve, "Distributed Massive MIMO Systems With Non-Reciprocal Channels: Impacts and Robust Beamforming," *IEEE Trans. Commun.*, vol. 66, no. 11, pp. 5261–5277, Nov. 2018.

[10] R. Rogalin, O. Y. Bursalioglu, H. Papadopoulos, G. Caire, A. F. Molisch, A. Michaloliakos, V. Balan, and K. Psounis, "Scalable Synchronization and Reciprocity Calibration for Distributed Multiuser MIMO," *IEEE Trans. Wireless Commun.*, vol. 13, pp. 1815–1831, Apr. 2014.

[11] M. Attarifar, A. Abbasfar, and A. Lozano, "Random vs structured pilot assignment in cell-free massive MIMO wireless networks," in *Proc. 2018 ICC Workshops*, May 2018, pp. 1–6.

[12] O. Raeesi, A. Gokceoglu, and M. Valkama, "Estimation and Mitigation of Channel Non-Reciprocity in Massive MIMO," *IEEE Trans. Signal Process.*, vol. 66, pp. 2711–2723, May 2018.

[13] C. Shepard, H. Yu, N. Anand, E. Li, T. Marzetta, R. Yang, and L. Zhong, "Argos: practical many-antenna base stations," in *Proc. MobiCom 2012*, Istanbul, Turkey, 2012, pp. 53–64.

[14] M. Guillaud, D. T. M. Slock, and R. Knopp, "A practical method for wireless channel reciprocity exploitation through relative calibration," in *Proc. ISSPA 2005*, vol. 1, Aug. 2005, pp. 403–406.

[15] "Channel Reciprocity Modeling and Performance Evaluation," in *TSG RAN WG164, R1-110804, Alcatel-Lucent*, Boulogne-Billacourt, France, 3GPP, 2010.

[16] E. Bjoernson, J. Hoydis, and L. Sanguinetti, "Massive MIMO Networks: Spectral, Energy, and Hardware Efficiency," *Found. and Trends in Signal Process.*, vol. 11, no. 3-4, pp. 154–655, 2017.

[17] H. Yang and T. L. Marzetta, "Performance of Conjugate and Zero-Forcing Beamforming in Large-Scale Antenna Systems," *IEEE J. Sel. Areas Commun.*, vol. 31, no. 2, pp. 172–179, Feb. 2013.

[18] Z. Chen and E. Bjoernson, "Channel Hardening and Favorable Propagation in Cell-Free Massive MIMO With Stochastic Geometry," *IEEE Trans. Wireless Commun.*, vol. 66, pp. 5205–5219, Nov. 2018.

[19] 3GPP, "Study on channel model for frequencies from 0.5 to 100 GHz," 3GPP, Tech. Rep. TR 38.901, Jun. 2018, Rev. 15.0.